

Suppression of Injection Bump Leakage Caused by Sextupole Magnets within Bump Orbit

**Hitoshi TANAKA¹, Takashi OHSHIMA, Kouichi
SOUTOME
and Masaru TAKAO**

**SPring-8/JASRI, 1-1-1 Kouto, Mikazuki-cho
Sayo-gun Hyogo 679-5198, Japan**

Aug. 14, 2004

**Submitted to Nuclear Instruments and Methods in Physics Research
Section A (NIM A),**

Nov. 01, 2004

Accepted by NIM A

Reference Number: BAR-04:115

¹ Corresponding author. Tel.: +81-791-58-0851; fax: +81-791-58-0850. E-mail address:

tanaka@spring8.or.jp (H. Tanaka)

Suppression of Injection Bump Leakage Caused by Sextupole Magnets within a Bump Orbit

Hitoshi TANAKA^a, Takashi OHSHIMA, Kouichi SOUTOME and Masaru
TAKAO

SPring-8/JASRI, 1-1-1 Kouto, Mikazuki-cho, Sayo-gun Hyogo 679-5198, Japan

Abstract: We propose a scheme to suppress leakage of an injection bump orbit caused by sextupole magnets within the bump orbit. Since the bump leakage excites a stored beam oscillation synchronized with beam injection, its suppression is one of the most crucial issues for achieving top-up operation at third generation synchrotron radiation (SR) sources. In the common case where sextupole magnets are located within the bump orbit, the condition for closing the bump depends on the amplitude of the bump orbit due to the nonlinear kicks by the sextupole magnets. Accordingly the bump orbit never closes for all amplitudes even under ideal condition. To solve this problem, we use a minimal condition for emittance increase due to the bump leakage caused by sextupole magnets in the lowest order of the nonlinear perturbation. The condition is obtained by optimizing linear optics and satisfying specific relation among integrated strengths of the sextupole magnets within the bump orbit. Furthermore, the condition does not depend on the bump amplitude. Calculations using the perfectly similar field patterns reveal that the proposed scheme can reduce the rms of the stored beam oscillation down to a few tens of microns for all bump amplitudes. The residual oscillation is negligibly small compared to the horizontal beam sizes presently achieved in the SR sources. The

^a Corresponding author. Tel.: +81-791-58-0851; fax: +81-791-58-0850. E-mail address:

tanaka@spring8.or.jp (H. Tanaka)

suppression effect of the scheme was also confirmed experimentally by the results obtained at the SPring-8 storage ring.

29.20.-c, 29.20.Dh, 29.27.-a, 29.27.Ac, 41.60.Ap, 41.85.Ar

1. Introduction

Recent performance improvements of synchrotron radiation (SR) sources increase stored beam density. Although the high density contributes to the generation of brilliant and coherent photon beams, it causes the problem of shortened beam lifetime from electron-electron scattering in a bunch even in high-energy SR sources such as the 8-GeV SPring-8^{1 2}. Thus, further low emittance conflicts with required long beam lifetime. The so-called top-up operation^{3 4} is a way to manage both the low emittance and the short beam lifetime.

In top-up operation, continuous beam injection at short intervals, e.g., 30 seconds, keeps the current approximately constant with a small current deviation, e.g., 0.1 %. This means that the beam lifetime averaged over the period longer than the injection interval is, in a sense, equal to infinity. However, when the beam injection excites an oscillation of the stored beam with amplitude larger than the beam size, the photon beam experiments are disturbed. The excited oscillation effectively enlarges the stored beam emittance and modulates the photon beam intensity. Suppression of the stored beam oscillation is therefore crucial for achieving the ideal top-up operation for experimental users and for making the most of third generation SR sources.

The main causes for the transverse oscillation of the stored beam are two-fold. One cause is bump magnet errors, which can involve variations in the field patterns of the bump magnets, differences of the magnet configuration, differences in the magnet boundary conditions, magnet misalignments and parameters of the equivalent circuit of the magnet including the coaxial cables, etc. These magnet errors can be solved in principle by engineering improvement. The other cause is nonlinearity within an injection bump orbit. In general, sextupole magnets can be found within the bump orbit of third generation SR sources because dynamic stability of the stored beam requires more sextupole magnets. These sextupole magnets make the closing bump condition depend on the bump amplitude. Thus the bump orbit never closes for all amplitudes even when all bump magnets are powered ideally. Furthermore, this nonlinear effect causes a large oscillation and is the dominant perturbation for SPring-8. A long straight section might make a nonlinearity-free bump orbit possible⁵. However, this solution is not easily applicable to existing and also to newly planned SR sources due to following reasons: (I) The necessary length for the injection gets longer as the stored beam energy is higher, (II) adoption of long straight sections increases the construction cost and causes large scale modification in existing SR sources, and (III) long straight sections are also valuable for generation of high quality radiation and development of new radiation sources.

To suppress the injection bump leakage by the sextupole magnets, we have investigated the condition for minimum emittance of the bump leakage in the lowest order of a nonlinear perturbation. In the case where amplitude of the bump orbit is small, on the order of 0.01 m, the lowest nonlinear order mainly contributes to the leakage. We found that the minimum condition in the lowest order of the perturbation does not depend on

the bump amplitude. This suggests that the optimization of the sextupole strengths can drastically reduce the oscillation excitation. The minimum condition is obtained by both optimizing the linear optics and satisfying a specific relation among integrated strengths of the sextupole magnets within the bump orbit.

We explain our suppression scheme in the next section and discuss its effect on the bump leakage in section 3. We then describe how to enlarge the dynamic stability while suppressing the bump leakage in section 4 and compare the calculation results with experimental ones for the case of SPring-8 in section 5.

2. Proposed suppression scheme

The suppression scheme we present here is that of the bump leakage caused by the lowest order of the nonlinear perturbation. As we see later, the lowest and second order perturbations work as dipole and quadrupole field errors, respectively and have the different dependences on the bump amplitude. By utilizing the different dependences, our scheme can suppress both contributions simultaneously. First we describe the bump leakage by the sextupole magnets when the orbit comprises of four bump magnets as shown in Fig. 1. The bump orbit is generated in the horizontal plane, and the strengths of the quadrupole, sextupole and bump magnets are symmetric with respect to the center of the straight section.

In the case where the strengths of all the sextupole magnets are zero, the closed bump amplitude at each sextupole magnet is expressed by

$$\begin{aligned}
x_{si} &= \sqrt{\beta_{si} \cdot \beta_{b1}} \cdot K_{b1} \cdot \sin(\phi_{si} - \phi_{K1}), \quad i = 1, 2, \\
x_{sj} &= \sqrt{\beta_{sj} \cdot \beta_{b4}} \cdot K_{b4} \cdot \sin(\phi_{K4} - \phi_{sj}), \quad j = 3, 4, \\
K_{b1} &= K_{b4} = \frac{(B_y L)_{b1}}{B\rho}, \quad \phi_{si} - \phi_{K1} = \phi_{K4} - \phi_{sj}, \quad \beta_{b1} = \beta_{b4},
\end{aligned} \tag{1}$$

where $(B_y L)_{b1}$ represents the integrated field strength of the first bump magnet B1 in Fig. 1. The parameters β and ϕ stand for the betatron function and the phase advance of a betatron oscillation, respectively. The suffixes si, sj and bi represent the i(j)-th sextupole and the i-th bump magnets shown in Fig. 1, respectively. When the bump orbit closes under the linear condition and the sextupole strengths are non-zero, leakage of the bump orbit at the fourth bump magnet B4 is expressed by

$$\begin{bmatrix} \Delta x_{b4} \\ \Delta x'_{b4} \end{bmatrix} = M_5 M_4 M_3 M_2 \cdot \begin{bmatrix} 0 \\ \Delta K_{s1} \end{bmatrix} + M_5 M_4 M_3 \cdot \begin{bmatrix} 0 \\ \Delta K_{s2} \end{bmatrix} + M_5 M_4 \cdot \begin{bmatrix} 0 \\ \Delta K_{s3} \end{bmatrix} + M_5 \cdot \begin{bmatrix} 0 \\ \Delta K_{s4} \end{bmatrix}, \tag{2}$$

where,

$$\begin{aligned}
\Delta K_{s1} &= \frac{1}{2} \cdot \lambda_1 \cdot x_{s1}^2, \\
\Delta K_{s2} &= \frac{1}{2} \cdot \lambda_2 \cdot (x_{s2} + M_2(1,2) \cdot \Delta K_{s1})^2, \\
\Delta K_{s3} &= \frac{1}{2} \cdot \lambda_3 \cdot (x_{s3} + M_3 M_2(1,2) \cdot \Delta K_{s1} + M_3(1,2) \cdot \Delta K_{s2})^2, \\
\Delta K_{s4} &= \frac{1}{2} \cdot \lambda_4 \cdot (x_{s4} + M_4 M_3 M_2(1,2) \cdot \Delta K_{s1} + M_4 M_3(1,2) \cdot \Delta K_{s2} + M_4(1,2) \cdot \Delta K_{s3})^2,
\end{aligned}$$

$$\lambda_i = \frac{\left(\frac{\partial^2 B_y}{\partial x^2} \cdot L \right)_{si}}{B\rho}, \quad i = 1 \sim 4, \quad \lambda_1 = \lambda_4, \lambda_2 = \lambda_3.$$

The parameter λ_i is the integrated strength of the i -th sextupole magnet normalized to the particle momentum with ΔK_{s_i} the horizontal kick, a function of the bump amplitude. The variables Δx and $\Delta x'$ represents the displacement and the angle of the orbit distortion, respectively. The symbol M denotes the 2 by 2 horizontal transfer matrix for the section between the two dashed lines in Fig. 1, and the numbers in the parentheses specify the matrix element.

2.1. Bump leakage caused by the lowest order sextupole perturbation

The injection bump orbit closes when both Δx_{b4} and $\Delta x'_{b4}$ are zero. One can see that Eq. (2) is a nonlinear equation in x_{s_i} up to the $16(2^4)$ -th power. Since the value of x_{s_i} is ~ 0.01 m and the matrix M_i is symplectic, we can treat x_{s_i} as a small perturbation. By approximating Eq. (2) in the lowest order of the perturbation, the horizontal kicks by each sextupole magnet are

$$\Delta K_{s1} = \frac{\lambda_1}{2} \cdot x_{s1}^2, \Delta K_{s2} = \frac{\lambda_2}{2} \cdot x_{s2}^2, \Delta K_{s3} = \frac{\lambda_3}{2} \cdot x_{s3}^2, \Delta K_{s4} = \frac{\lambda_4}{2} \cdot x_{s4}^2, \quad (3)$$

and the Δx_{b4} and $\Delta x'_{b4}$ contain only quadratic terms of K_{b1} . This holds even when the injection bump is an asymmetric case, because K_{b4} is proportional to K_{b1} .

Equation (2) also shows that the leakage-free condition is determined at the fourth sextupole magnet S4, not at the fourth bump magnet B4. This means that the orbit distortion by the sextupole magnets has to be self-compensating between S1 and S4 to close the bump completely. The position and the angle of the orbit distortion at S4, Δx_{s4}

and $\Delta x'_{s4}$ generate the bump leakage and they are obtained by multiplying Eq. (2) by the inverse matrix of M_5 from the left. With Δx_{s4} and $\Delta x'_{s4}$, one can write the emittance of the bump leakage caused by the lowest order of the perturbation $\Delta \varepsilon$ as

$$\Delta \varepsilon = \beta_{s4} \cdot \Delta x'^2_{s4} + 2\alpha_{s4} \cdot \Delta x_{s4} \Delta x'_{s4} + \gamma_{s4} \cdot \Delta x^2_{s4}, \quad (4)$$

where,

$$\Delta x_{s4}, \Delta x'_{s4} \propto K_{b1}^2, \quad \alpha_{s4} \equiv \frac{-1}{2} \cdot \frac{d\beta_{s4}}{ds}, \quad \gamma_{s4} \equiv \frac{1 + \alpha_{s4}^2}{\beta_{s4}}.$$

The optimum strength of each sextupole satisfies the condition that the partial derivative of the emittance by each sextupole strength is zero, which is given by

$$\frac{\partial \Delta \varepsilon}{\partial \lambda_i} = \frac{\partial \Delta x_{s4}}{\partial \lambda_i} \cdot (\gamma_{s4} \cdot \Delta x_{s4} + \alpha_{s4} \cdot \Delta x'_{s4}) + \frac{\partial \Delta x'_{s4}}{\partial \lambda_i} \cdot (\beta_{s4} \cdot \Delta x'_{s4} + \alpha_{s4} \cdot \Delta x_{s4}) = 0. \quad (5)$$

Since all the terms of each partial derivative depend on the 4th power of K_{b1} , Eq. (5) gives the optimum condition, which is independent of the bump amplitude. This means that the lowest order of the perturbation causes a leakage equivalent to that generated by a dipole field error. Equation (5) can be solved in general and defines the optimum strengths of the sextupole magnets. Actually the optimum condition given by Eq. (5) can be simplified by adjusting the linear optics. In the case where the absolute value of α_{s4} is much larger than unity, Eq. (5) can be approximated with $\gamma_{s4} \approx \alpha_{s4}^2/\beta_{s4}$ as

$$\frac{\partial \Delta \varepsilon}{\partial \lambda_i} = \left(\frac{\alpha_{s4}}{\beta_{s4}} \cdot \frac{\partial \Delta x_{s4}}{\partial \lambda_i} + \frac{\partial \Delta x'_{s4}}{\partial \lambda_i} \right) \cdot (\beta_{s4} \cdot \Delta x'_{s4} + \alpha_{s4} \cdot \Delta x_{s4}) = 0. \quad (6)$$

The optimum condition for the minimum leakage is obtained:

$$\Delta x'_{s4} = -\frac{\alpha_{s4}}{\beta_{s4}} \cdot \Delta x_{s4} . \quad (7)$$

which is a form independent of the sextupole family. Equation (7) gives a simple linear relation among integrated strengths of the sextupole magnets within the bump orbit. In the case shown in Fig. 1, the above relation defines the optimum ratio between integrated strengths of two sextupole families, λ_1 and λ_2 as

$$\frac{\lambda_2}{\lambda_1} = -\frac{\beta_{s1} \sin(\phi_{s1} - \phi_{K1})^2 \cdot \left[1 + \frac{\alpha_{s4}}{\beta_{s4}} M_4 M_3 M_2(1,2) + M_4 M_3 M_2(2,2) \right]}{\beta_{s2} \sin(\phi_{s2} - \phi_{K1})^2 \cdot \left[\frac{\alpha_{s4}}{\beta_{s4}} \{M_4 M_3(1,2) + M_4(1,2)\} + M_4 M_3(2,2) + M_4(2,2) \right]} . \quad (8)$$

2.2. Contribution from second order of sextupole perturbation

The second order of the sextupole perturbation in Eq. (2) appears as terms in the third power of K_{b1} and results in linear terms of K_{b1} in Eq. (7) when Eq. (7) is truncated at the second order of the perturbation. This also means that the second order of the perturbation excites a leakage equivalent to that generated by a quadrupole field error, which linearly depends on the bump amplitude. This kind of leakage may be compensated by adjusting strengths of the bump magnets.

2.3. Suppression scheme

SR sources typically suppress the leakage pragmatically by adjusting only the strengths of the bump magnets to close the bump orbit at the peak amplitude. This is because strengths of the sextupole magnets are predetermined according to the dynamic stability

of the stored beam, i.e., the sextupole strengths within the bump orbit are not free parameters but given. Consequently, the bump leakage by the lowest order of the perturbation remains significant. It is impossible to control both the lowest and second orders of the sextupole perturbation by tuning only the strengths of the bump magnets.

On the other hand, in our scheme, the bump leakage in the lowest order of the perturbation is suppressed by optimizing the linear optics at the sextupole magnets within the bump orbit and their strengths. In addition, the leakage in the second order of the perturbation is suppressed by adjusting strengths of the bump magnets without harming the first condition. Here, the strengths of the sextupole magnets within the bump orbit are set to minimize the leakage. The optimum condition for the leakage suppression requires only the relation among strengths of the sextupole magnets.

3. Calculation of suppression effect on injection bump leakage

We estimate the effect of the proposed scheme on reducing the injection bump leakage, i.e., reduction of the stored beam oscillation by using the identical half-sine field patterns. In the calculation, the mirror symmetric arrangement of four bump magnets as shown in Fig. 1 was used. Within the bump orbit there are two sextupole families, S1 (=S4) and S2 (=S3) with integrated strengths λ_1 and λ_2 , respectively. To simplify the problem, the bump pulse width is made shorter than the revolution period of the ring, which was assumed to be 3 μ sec. The Twiss parameters assumed are listed in Table 1. The absolute value of α_{s4} is tuned to be 6.5, which is much larger than unity, and accordingly the condition for the minimum leakage is given to a good approximation by Eq. (7).

3.1. Numerical calculations

Since amplitude of the bump leakage is expected to be small, being at most a few mm, we can neglect all the higher-order effects due to nonlinear fields, a longitudinal oscillation, etc. outside the injection bump orbit. A main source of a nonlinear perturbation inside the bump orbit is a sextupole magnet from the viewpoint of the bump leakage. These thus justify the use of a simple ring-simulator composed of linear elements, sextupole magnets, injection bump magnets and beam position monitors (BPMs) in numerical calculations.

The simulator is a simple four dimensional kick-code where transverse motion is only traced by transfer matrices and nonlinear kicks. In the simulator drift spaces, bending and quadrupole magnets are treated as linear elements and a conventional 4 by 4 transfer matrix gives particle motion over each element. All sextupole magnets are treated as thin lenses and the particle motion over the sextupole magnet is calculated with an integrated nonlinear kick at the centre of the magnet. The BPM arrangement is reconstructed in the simulator and each BPM stores the horizontal and vertical positions of a test particle turn by turn. All injection bump magnets are also treated as thin lenses with time-dependent kicks generated by a predefined table. These values were taken from experimental field data measured by using a search-coil or simply calculated with an ideal sinusoidal function depending on our purpose of calculations. The trajectory of the test particle is traced along the ring by kicking the particle at each bump magnet according to the table of the kick data. We thus obtain the rms oscillation amplitude of the stored beam caused by the bump leakage for one particle with specified timing against the bump excitation. By repeating the timing-shift to scan all RF-buckets, the

rms oscillation amplitude is obtained as a function of the stored beam position along the ring.

3.2. Bump leakage at minimum condition

The analysis based on the lowest order of the perturbation predicts that R , the ratio of λ_2 to λ_1 , determines the bump leakage. By using Table 1 data and Eq. (8) we obtain $R=-0.57$ as the optimum R that gives the minimum bump leakage. To verify the prediction, we investigate the minimum condition numerically by using the bump orbit closure under the linear condition whose peak amplitude is 14.5 mm at the injection point. Figure 2 shows the rms oscillation amplitude of the stored beam calculated by using λ_2 as a parameter together with the bump field pattern normalized by its peak value. Here, λ_1 was fixed to -1.5 m^{-2} . The horizontal axis represents the phase of the bump pulse τ in μsec , which is related to the phase angle θ through $\theta = \pi \times (\tau/3)$. The bump amplitude is zero at both 0 and 3 μsec and it takes the maximum value of 14.5 mm at 1.5 μsec . The vertical axis represents x_r which is the rms value of the excited stored beam oscillation. We see that the bump leakage at all the phases from 0 to 3 μsec takes the minimum values around the condition that λ_2 is 0.86 m^{-2} , which corresponds to $R=-0.57$. This result agrees well with the prediction by the analysis based on the lowest order of the perturbation.

We also investigated the dependence of the bump leakage on the ratio R by changing λ_1 from -1.5 to -4.5 m^{-2} . Figure 3 shows the calculated results. The vertical axis represents x_{2r} , which is the rms value of the excited beam oscillation averaged over both the phase

of the bump pulse and the betatron phase of the excited oscillation. The solid lines represent the fitted results by the following function assuming linearity:

$$x_{2r} = S_E \times |R - R_{\min}| + x_{2r_min}, \quad (9)$$

where x_{2r_min} and R_{\min} are the minimum of the rms oscillation amplitude x_{2r} and the ratio R at the minimum, respectively. The coefficient S_E represents the sensitivity of the excited rms amplitude against the deviation from the optimum value. We see that the minimum condition lies in the narrow range of R from -0.57 to -0.61. This result agrees with the prediction that the minimum condition does not depend on the absolute strengths of the sextupole magnets.

In Fig. 4, the values of S_E , x_{2r_min} and R_{\min} obtained are plotted against λ_1 . In the range where λ_1 is from -1.5 to -4.5 m⁻², we see that the rms value of the excited oscillation can be suppressed to less than 20 μm . We also find that the fitted R_{\min} gradually deviates from the prediction as the absolute value of λ_1 increases. The calculated oscillation amplitude involves contributions from all orders of the perturbation, whereas the prediction is based only on the lowest order. The higher order terms naturally increase with the absolute value of λ_1 and these terms cause the deviation from the predicted ratio.

3.3. Effect of adjusting strengths of bump magnets for bump closure at peak amplitude

To suppress the injection bump leakage, strengths of the bump magnets are usually adjusted so as to close the bump orbit at the peak amplitude. This treatment efficiently corrects the second order of the perturbation. We thus combined the correction of the lowest order of the perturbation with the conventional strength adjustment of the bump magnets. Figure 5 shows the rms amplitude of the excited oscillation calculated using λ_2 as a parameter with λ_1 fixed at -3.5 m^{-2} . In this calculation, strengths of the bump magnets were adjusted to close the bump at the peak amplitude for each set of the sextupole magnets. For comparison, the calculation without the strength adjustment is also shown for the case of $\lambda_1 = -3.5 \text{ m}^{-2}$ and $\lambda_2 = 1.2 \text{ m}^{-2}$. We see that the bump leakage reaches a minimum when R is around -0.63 . The rms oscillation is also suppressed down to a few tens μm . The fitted $x_{2r-\text{min}}$ is about $10 \mu\text{m}$ for $\lambda_1 = -3.5 \text{ m}^{-2}$ and is almost the same as that by the correction of only the lowest order perturbation. Although the strength adjustment of the bump magnets is effective in reducing S_E in Eq. (9), it does not lower the achievable minimum notably. This fact shows that the lowest order perturbation is dominant in the bump leakage.

4. Recovery of dynamic stability

In general a dynamic aperture (DA) of a ring accelerator must be large enough for stable beam injection. It is, however, difficult to realize sufficiently large DA for a low-emittance SR source. This is mainly due to strong sextupole magnets used for correcting large linear chromaticity. These strong magnets markedly excite harmful systematic resonance lines such as $\nu_x = N$, $3\nu_x = N$, $\nu_x \pm 2\nu_y = N$, where ν_x and ν_y are the horizontal

and vertical betatron tunes, respectively, and N is a multiple of the ring periodicity. To enlarge the DA, keeping the linear chromaticity correction unchanged, additional sextupole magnets in dispersion-free sections are usually introduced to suppress the harmonics that drive the harmful resonance lines⁶. For this reason several sextupole families are provided in the low-emittance SR sources.

As explained in section 2, the analysis based on the lowest order of the perturbation gives the relation among strengths of the sextupole magnets (see Eq. (8)). This relation does not guarantee the optimum condition for the above harmonic suppression. Hence, when the optimum condition for the leakage suppression is applied to sextupole magnets inside the injection bump orbit, some systematic resonance lines are excited and they possibly reduce the DA. The reduction of the DA, however, can be recovered by re-suppressing the excited resonance lines with additional sextupole magnets outside the injection bump orbit. The recovery of the DA is therefore consistent with the leakage suppression. In the following, taking the SPring-8 storage ring as an example, we explain how to enlarge the DA preserving the optimum condition for the leakage suppression.

The SPring-8 storage ring comprises of 36 Chasman Green (CG) unit cells and 4 long straight sections (LSSs) with matching parts at both ends⁷. The strength distribution of the sextupole magnets is mirror symmetric in one CG unit cell and the distribution was originally determined to maximize the DA. Under this condition, four degrees of freedom were available for strength optimization of the sextupole magnets. When we suppress the bump leakage, one degree of freedom is used for the leakage suppression and two of the remaining ones are used for the linear chromaticity correction. This implies that there is little room for DA enlargement. Figure 6 shows the dependence of the horizontal DA

on R , the ratio of λ_2 to λ_1 using λ_1 as a parameter. Particle tracking is started with an initial betatron phase of π and the X-Y coupling of 1 % from the beam injection point of which β_x and β_y are 23m and 6.4m, respectively. Here, only one CG unit cell was used to simplify the calculation and horizontal and vertical chromaticities were set to +8. We see that the optimum ratio for the DA is far from the $R_{\min} = -0.57$ condition shown by the broken line. In addition the DA is small around R_{\min} , with a value of only 15 mm at the beam injection side. Since the oscillation amplitude of the injected beam is about 10 mm and both magnetic errors and insertion of LSSs reduce the DA, 15 mm is too small to achieve a stable beam injection condition.

A method to bring additional degrees of freedom for the DA enlargement is to expand the unit structure of the ring. By expanding the unit structure from one CG cell to two cells as shown in Fig. 7, the degree of freedom increases from four to six for the SPring-8 storage ring and new two degrees of freedom, S5 and S6 in Fig. 7, are available for the DA enlargement. By optimizing strengths of the sextupole magnets under this new situation, the DA is increased by a factor of two as shown in Fig. 8, which is large enough for the stable beam injection. In this calculation, the full storage ring structure without magnetic errors was used.

The effectiveness of the above scheme was checked experimentally by measuring injection efficiency before and after the DA enlargement. We first measured the injection efficiency for the case of the four sextupole families shown in Fig. 7(A). The measured efficiency was about 5 %. To improve this low efficiency, cabling change of the sextupole magnets was carried out in the summer 2003 to realize the expansion of the

unit structure of the ring. The new cabling enables us to make use of the six sextupole families shown in Fig. 7(B). By optimizing strengths of these six sextupole families, the injection efficiency was markedly improved and more than 80 % was achieved.

5. Experimental results for suppression of injection bump leakage

We investigated the effect of the proposed suppression scheme experimentally in the SPring-8 storage ring. Four pulse bump magnets arranged almost the same way as shown in Fig. 1 generate the injection bump orbit. The strengths of the four bump magnets are adjusted so that the bump orbit closes at the peak amplitude. The bump pulse-width is 8.2 μsec , which is larger than the revolution period of 4.79 μsec . This means that the bump magnets kick a major part of the stored beam twice. Two families of sextupole magnets are located within the bump orbit and their arrangement is also the same as shown in Fig. 1. The absolute value of α_{s4} , a critical parameter, is larger than 6 owing to the characteristic arrangement of quadrupole magnets in the CG unit cell. This large α_{s4} guarantees that the condition for the minimum leakage is given by Eq. (7). The results obtained in section 3 shows that the optimum value of R is -0.63.

Figure 9 shows the measured field patterns. The clear variations in the patterns are seen at the rising and falling parts of the pulses. These cause the stored beam oscillation, which can not be reduced by the proposed suppression scheme. Using these measured field patterns, the suppression effect was calculated by scanning R from -0.57 to -0.81, and shown in Fig. 10. We see that the oscillation originating from the sextupole nonlinearity is markedly reduced with $R=-0.63$ as predicted by the analysis with the lowest perturbation. For the same range of the ratio R , we measured the dependence of

the rms horizontal oscillation amplitude on the phase of the pulse bump by using 276 single-pass beam position monitors. Figure 11 shows the experimental results. A comparison between Figs. 10 and 11 shows that the measurement agrees well with the calculation. In two cases for $R=-0.63$ and $R=-0.57$, the calculated reductions are smaller compared with the measured ones especially after ~ 10 μsec . The field measurement error around the under-shoot part is probably reasonable for this difference, because the calculation explains well the measurement in the period from 0 to 8 μsec , which is not affected by the under-shoot part.

6. Summary

We propose a scheme to suppress the injection bump leakage caused by sextupole magnets within the bump orbit. The proposed scheme is based on suppression of the lowest order of the sextupole perturbation. Since this perturbation works as a dipole field error, the excited oscillation is suppressed for all bump amplitudes by optimizing both the linear optics and the strengths of sextupole magnets within the injection bump. This scheme can reduce the amplitude of the excited oscillation down to a few tens of μm rms even though the scheme is quite simple and needs no significant modification of the magnet arrangement. The residual oscillation is negligibly small compared to the horizontal beam sizes presently achieved in the third generation SR sources. In other words, the stored beam oscillation will become invisible for experimental users under the proposed scheme. To verify the suppression effect experimentally, the reduction of the stored beam oscillation by the proposed scheme was measured at SPring-8. Through the comparison between the calculated and measured results, the effectiveness of the scheme was confirmed. We conclude that the proposed scheme is useful for suppressing the

injection bump leakage caused by the sextupole magnets and aids effective top-up operation at the third generation SR sources.

7. Acknowledgement

The authors wish to thank Dr. N. Kumagai and Dr. H. Ohkuma for their support and continuous encouragement. They would also like to express their sincere thanks to Dr. Louis Emery of the Advanced Photon Source who carefully read the manuscript and revised the English especially.

8. References

¹ H. Kamitsubo, Nucl. Instr. and Meth. **A303**, 421 (1991).

² Conceptual Design Report, SPring-8 Project part I Facility Design 1991 [Revised], JAERI-RIKEN SPring-8 Project Team (1991).

³ Conceptual Design Report, ANL-87-15 (1987).

⁴ S. Nakamura, M. Ohno, N. Awaji, A. Chiba, R. Kitano, H. Nishizawa, O. Asai, M. Takanaka, T. Iida, Y. Yamamoto, M. Shiota, M. Mizota, S. Kawazu, M. Kodaira, K. Kondo, and T. Tomimasu, 2nd European Particle Accelerator Conference, Nice, 472, (1990), edited by P. Marin and P. Mandrillon Editions Frontières, Gif-sur-Yvette, (1990).

⁵ M. Böge, H. U. Boksberger, M. Busse-Gravitz, M. Dehler, D. Dohan, D. George, C. H. Gough, S. Hunt, W. Joho, P. Marchand, G. Mülhaupt, L. Rivkin, V. Schlott, L. Schulz, A. Streun, P. Wiegand, F. Wei, A. Wrulich, and J. A. Zichy, 6th European Particle Accelerator Conference, Stockholm, 623, (1998), edited by S. Myers, L. Liljeby,

Ch. Petit-Jean-Genaz, J. Poole, K.-G. Rensfelt Institute of Physics Publishing, Bristol and Philadelphia, (1998).

⁶ E. A. Crosbie, IEEE Particle Accelerator Conference, Washigton, D. C., 443, (1987), edited by E. R. Lindstrom, L. S. Taylor IEEE, Piscataway, (1987).

⁷ H. Tanaka, K. Soutome, M. Takao, M. Masaki, H. Ohkuma, N. Kumagai, and J. Schimizu, Nucl. Instr. and Meth. **A486**, 521 (2002).

Fig. 1 Arrangement of the injection bump magnets. The injection bump orbit generated by the bump magnets (B1~B4, the empty squares) contains two bending magnets (BMs, the hatched squares), six quadrupole magnets (Qs, the filled rectangles), and the sextupole magnets (S1~S4, the empty rectangles). The symbol M denotes the horizontal transfer matrix for the section between the two dashed lines.

Fig. 2 Rms oscillation amplitude x_r versus the phase of the pulse bump τ when the bump orbit closes under purely linear condition. The sextupole strength λ_1 is set to be -1.5 m^{-2} and λ_2 is changed as a parameter from $+0.6$ to $+1.2$.

Fig. 3 Rms oscillation amplitude averaged over both the oscillation and the pulse bump phases x_{2r} versus R the ratio of λ_2 to λ_1 . The lines denote the fitted results with Eq. (9). The broken line denotes R_{\min} predicted by the analysis based on the lowest order of the perturbation.

Fig. 4 Fitting parameters, R_{\min} , x_{2r} , and S_E versus R the ratio of λ_2 to λ_1 .

Fig. 5 Rms oscillation amplitude x_r versus the phase of the pulse bump τ when the bump orbit closes at the maximum bump amplitude. The sextupole strength λ_1 is set to be -3.5 m^{-2} and λ_2 is changed as a parameter from $+1.2$ to $+2.5$.

Fig. 6 Horizontal dynamic apertures for the SPring-8 storage ring without errors versus R the ratio of λ_2 to λ_1 . The sextupole strength λ_1 is changed as a parameter from -3.0 to -4.0 . The broken line shows the optimum R for the suppression of the bump leakage.

Fig. 7 Expansion of the unit structure of the ring. The unit composed of 1 CG cell (A) has four sextupole families and the symmetry point located at the center of the CG cell as shown by the broken line. By expanding the unit from 1 to 2 CG cells (B), sextupole families can be increased up to six.

Fig. 8 Comparison of the ideal dynamic apertures for the SPring-8 storage rings with the different numbers of sextupole families. The open and filled circles show the dynamic aperture for the ring with 4 sextupole families and that with 6 sextupole families, respectively. In both cases the R is -0.57 with $\lambda_1=-3.5$ and $\lambda_2=2.0$. Particle tracking is started from the beam injection point.

Fig. 9 Measured field patterns of the four bump magnets installed in the SPring-8 storage ring.

Fig. 10 Rms oscillation amplitude x_r calculated with the measured field patterns of the pulse bump shown in Fig. 9.

Fig. 11 Rms oscillation amplitude x_r the measured at the SPring-8 storage ring.

Table 1 Twiss parameters at the sextupole and pulse bump magnets. Center of B1 is the reference of the phase advance.

Position	β_x [m]	α_x	ϕ_x [rad]
B1	3.67	1.42	0
S1	16.9	-6.50	2.21
S2	26.6	2.67	2.29
B2	22.9	0.13	2.34
B3	22.9	-0.13	2.41
S3	26.6	-2.67	2.46
S4	16.9	6.50	2.54
B4	3.67	-1.42	4.75

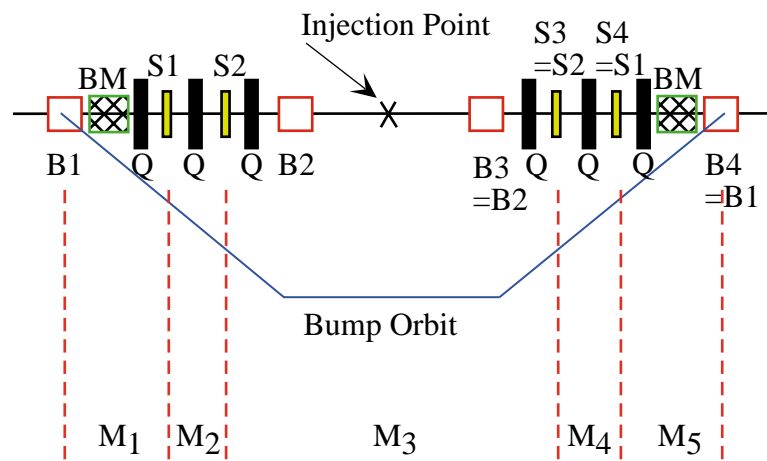


Fig. 1

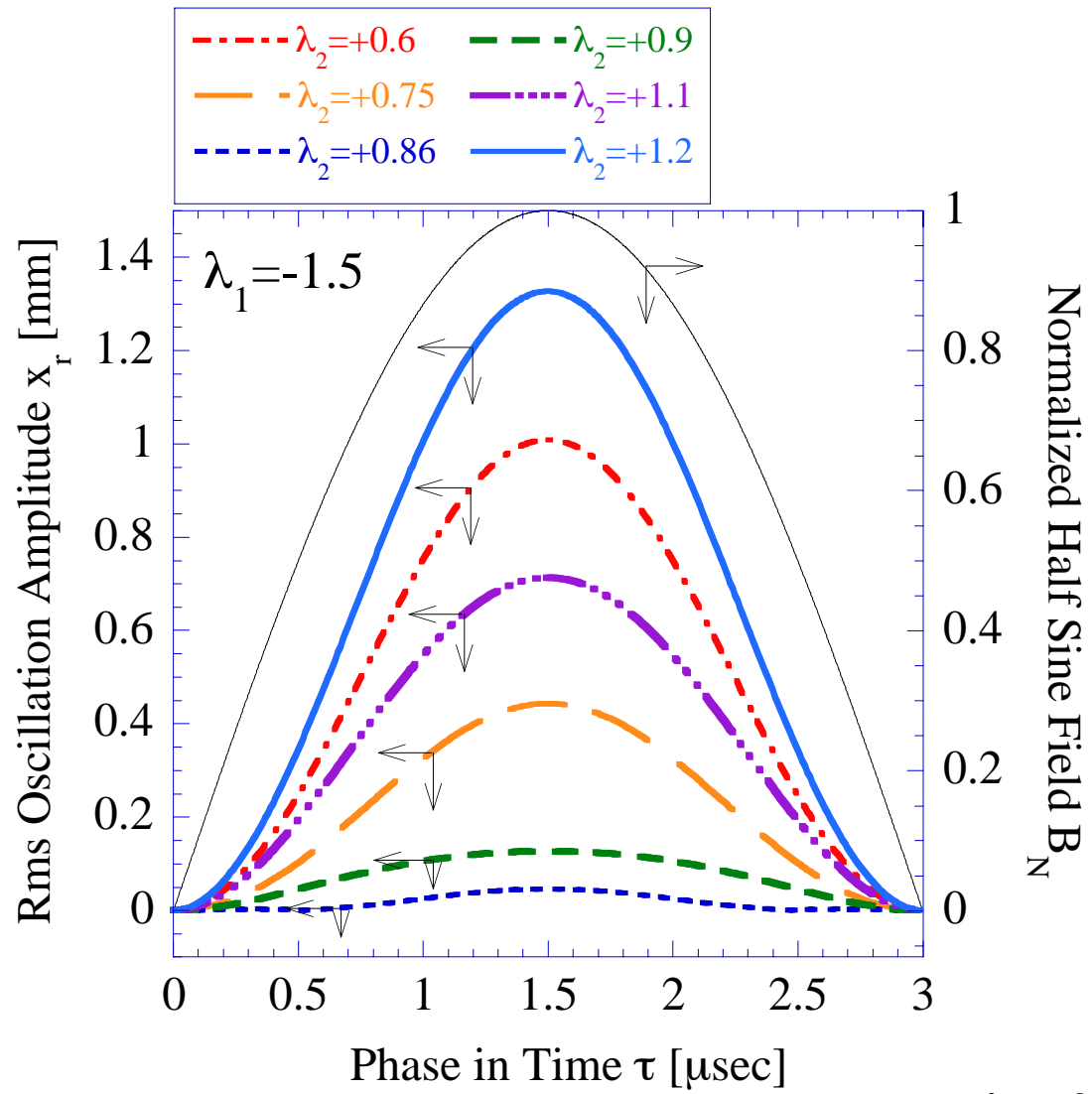


Fig. 2

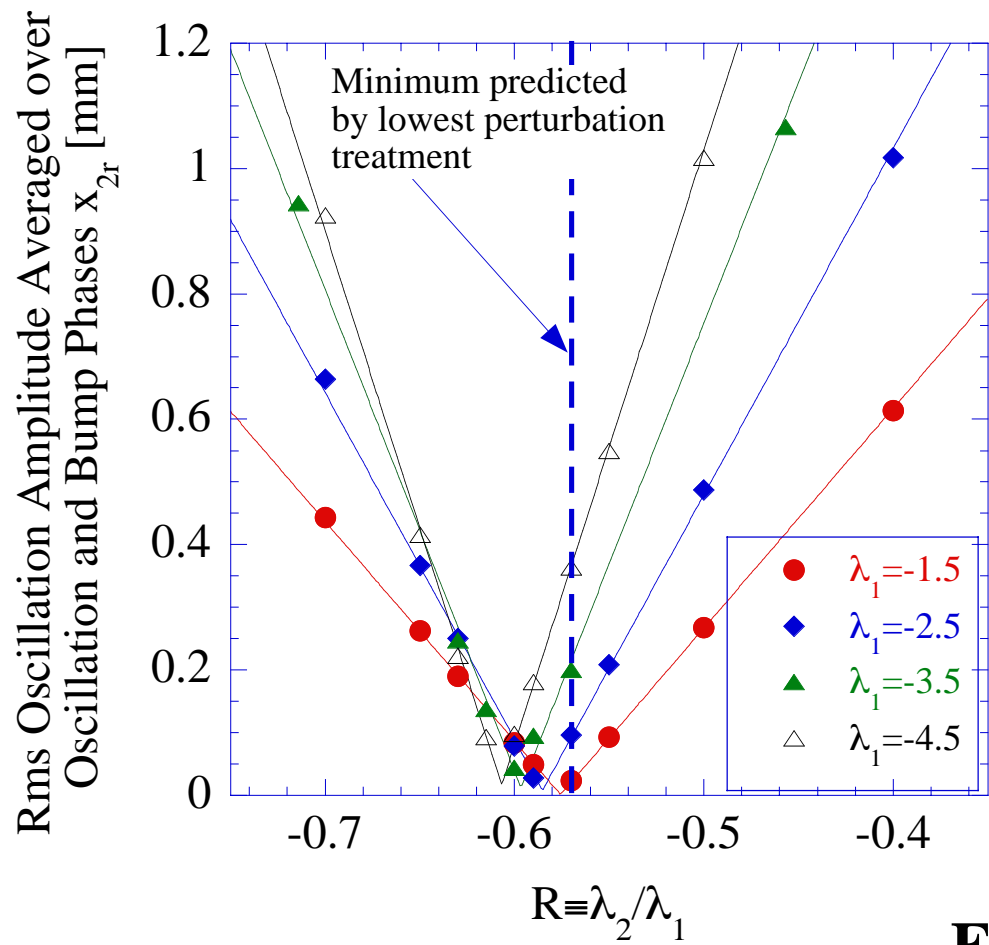


Fig. 3

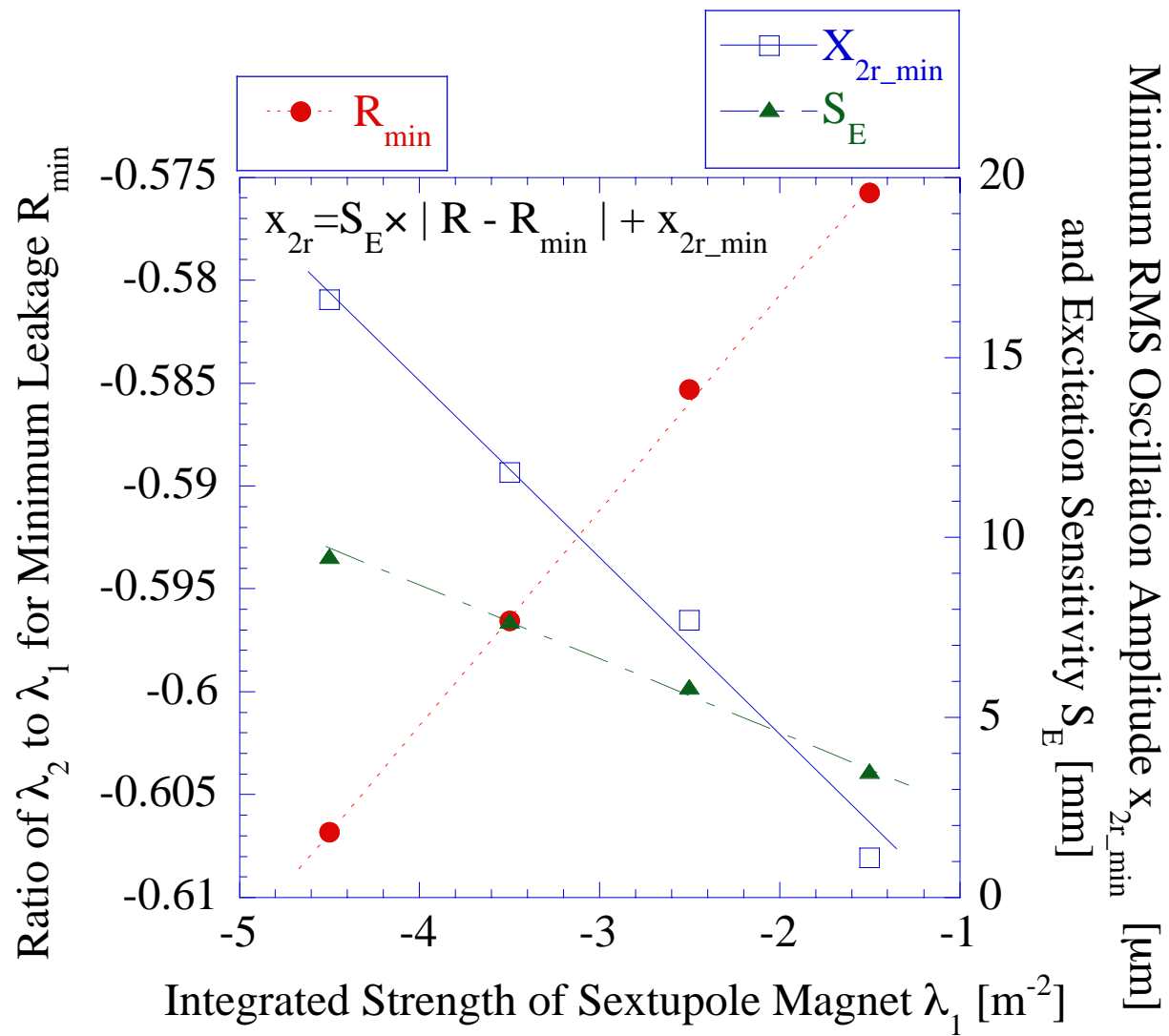


Fig. 4

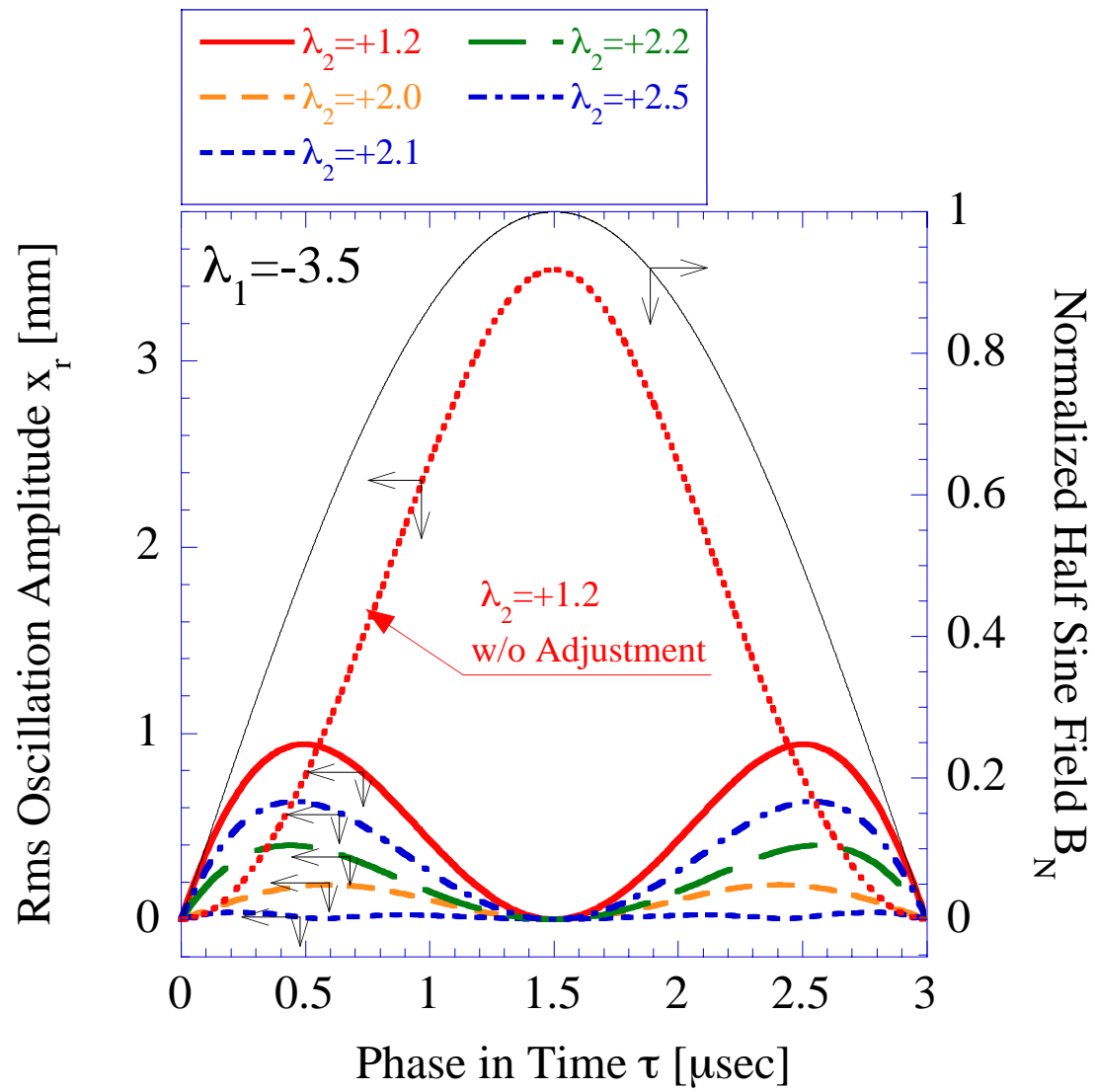


Fig. 5

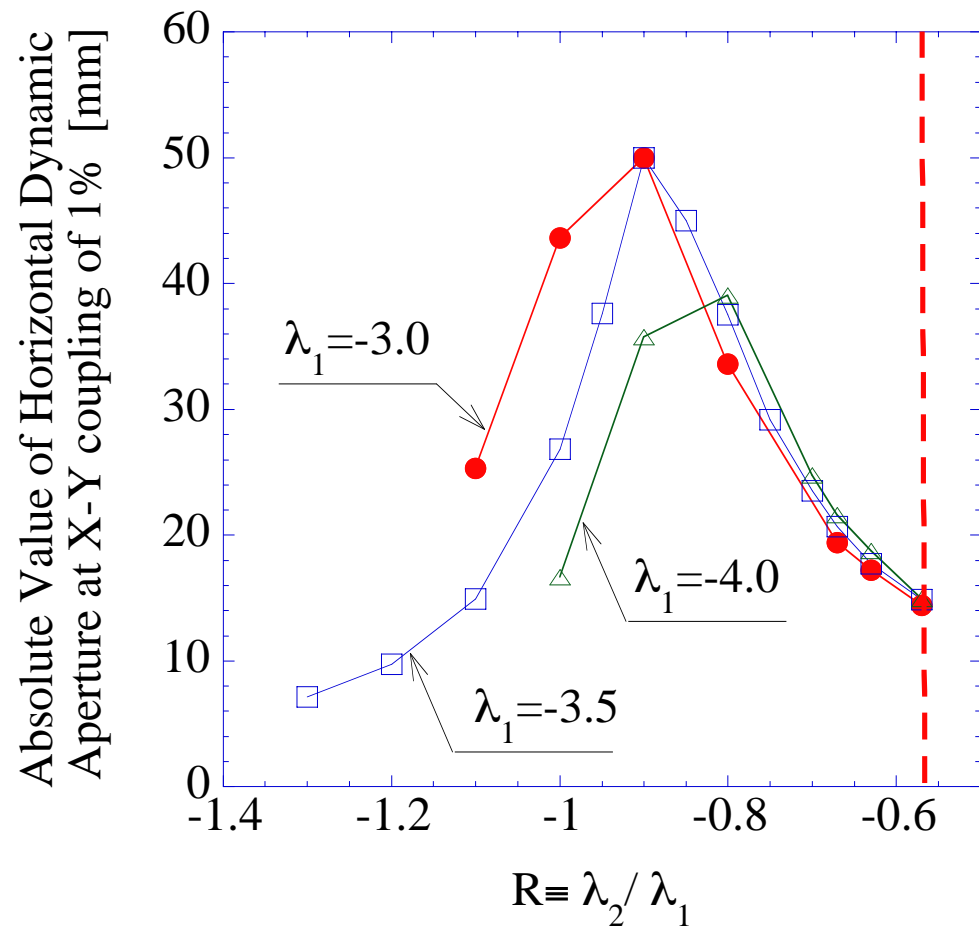
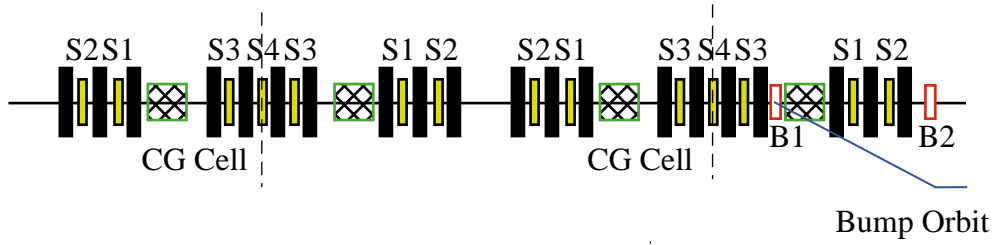


Fig. 6

(A) Unit Structure: 1CG Cell



(B) Unit Structure: 2CG Cells

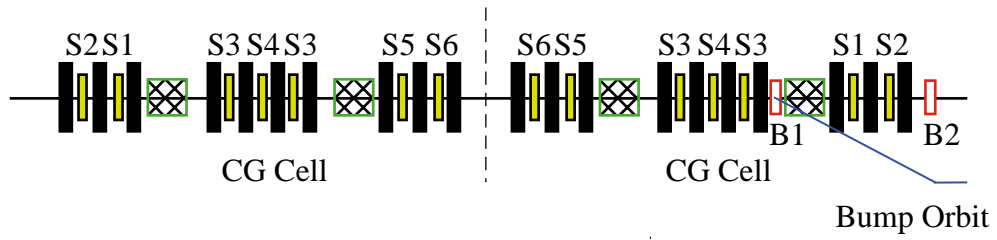


Fig. 7

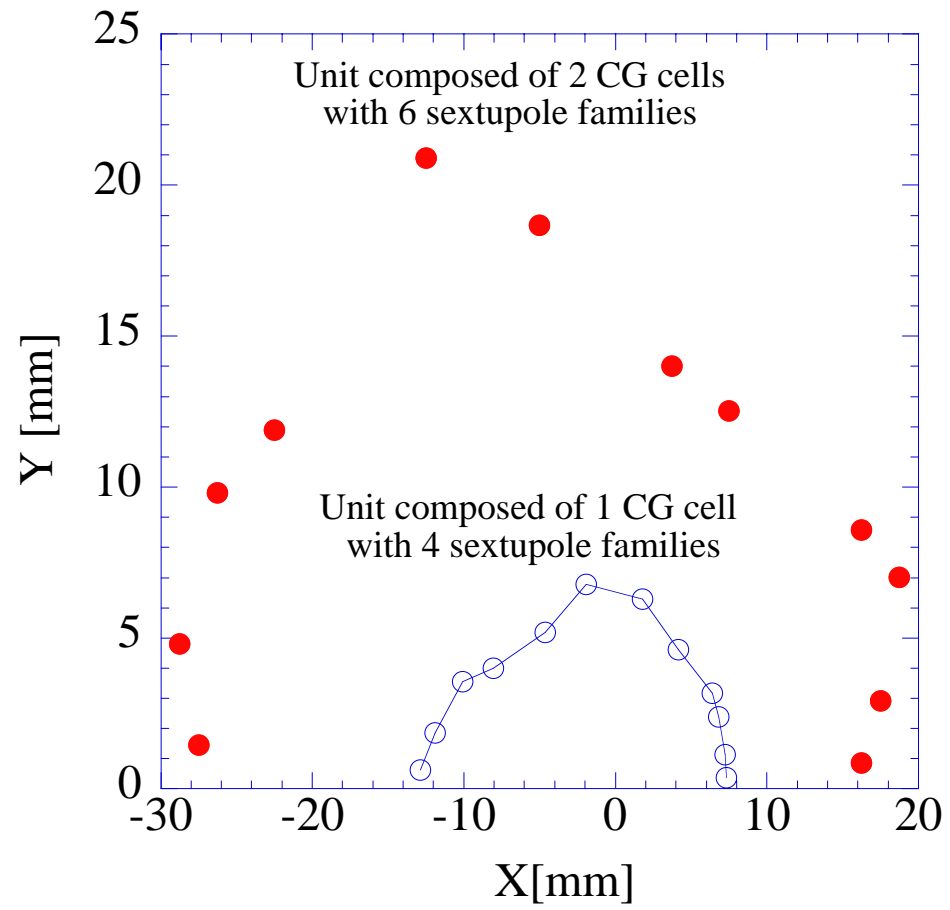


Fig. 8

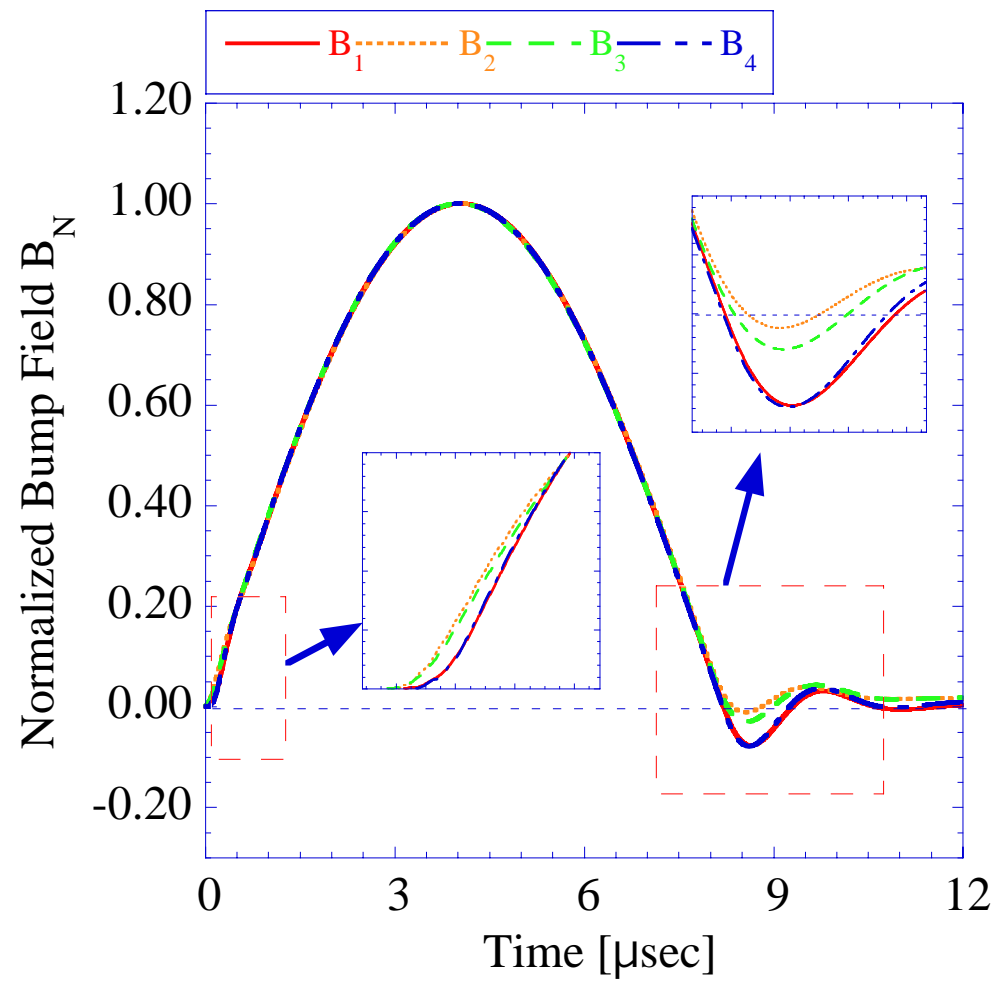


Fig.9

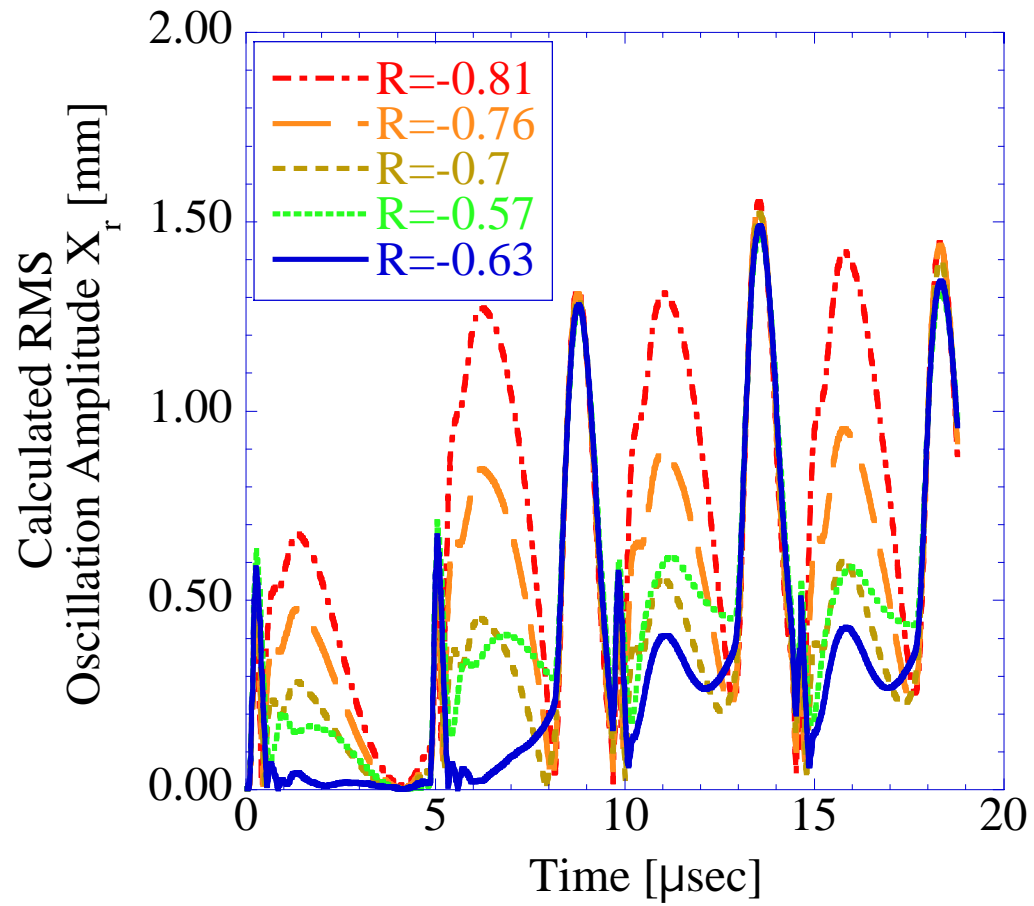


Fig. 10

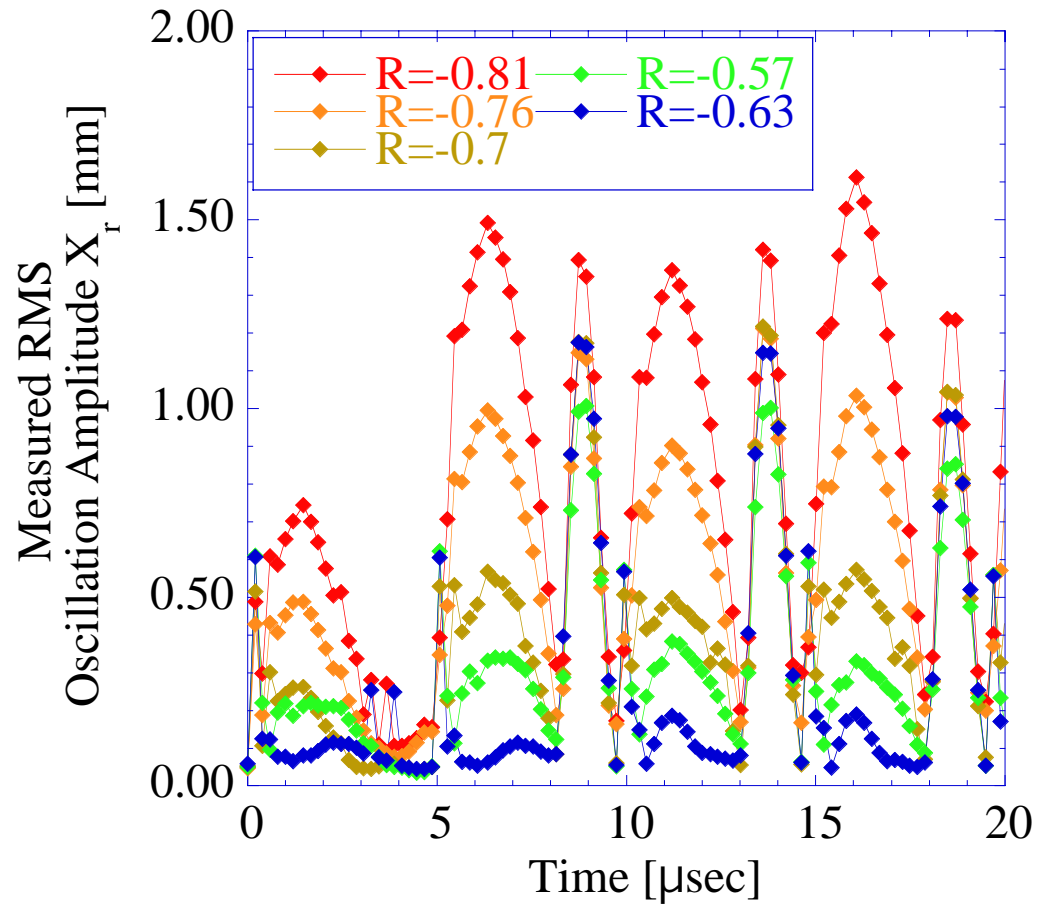


Fig. 11